blood advances

American Society of Hematology
2021 L Street NW, Suite 900,
Washington, DC 20036
Phone: 202-776-0544 | Fax 202-776-0545
bloodadvances@hematology.org

Targeting Neutrophil Extracellular Trap under Flow in Patients with Immune-Mediated Thrombotic Thrombocytopenic Purpura

Tracking no: ADV-2023-011617R3

Noritaka Yada (University of Kansas Medical Center, United States) Quan Zhang (University of Kansas Medical Center, United States) Antonia Bignotti (Unversity of Kansas Medical Center, United States) Sarah Gralnek (Unversity of Kansas Medical Center, United States) Dennis Sosnovske (University of Kansas Medical Center, United States) Keenan Hogan (University of Kansas Medical Center, United States) Zhan Ye (University of Kansas Medical Center, United States) Liang Zheng (University of Kansas Medical Center, United States) X. Long Zheng (University of Kansas Medical Center, United States)

Abstract:
Neutrophil NETosis is a unique form of cell death, characterized by release of decondensed chromatin and anti-microbial contents to the extracellular space, involved in infection, inflammation, and thrombosis. However, the role of NETosis in pathogenesis of immune-mediated thrombotic thrombocytopenic purpura (iTTP) and how a targeted therapy affects the accumulation of neutrophil extracellular traps (NETs) under flow remain to be determined. Flow cytometry demonstrated that the percentage of neutrophils undergoing NETosis in whole blood from iTTP patients on admission is significantly increased with a concurrent decrease in the capacity of inducible NETosis by shigatoxin. Following therapy, the percentage of H3Cit+MPO+ neutrophils was significantly reduced with an improvement of inducible NETosis in these patients. Additionally, little to no NET and thrombus formation was detected under flow in whole blood from iTTP patients when platelet counts were very low, but the NET and thrombus formation were dramatically increased following therapy when platelet count rose to □50x109/L or was restored to normal with donor platelets. Similarly, there was no thrombus and NET accumulation under flow in whole blood from vwf-/- mice, but NET accumulation was significantly higher in Adamts13-/- than wild-type mice. Finally, recombinant ADAMTS13 or caplacizumab (or anfibatide) prevents the NET and thrombus formation under flow in whole blood from iTTP patients (or Adamts13-/- mice). These results indicate that neutrophil NETosis and NET formation depend on platelets and VWF in iTTP, and a targeted therapy such as recombinant ADAMTS13 or caplacizumab may prevent the NET and thrombus formation under flow in iTTP.

Conflict of interest: COI declared - see note

COI notes: X.L.Z. is a speaker and/or consultant for Alexion, Sanofi, Takeda, Apollo, GC Biopharma, and Stago. X.L.Z. is also the co-founder of Clotsolution. All other authors have declared no relevant conflict.

Preprint server: No;

Author contributions and disclosures: N.Y. Q.Z., and X.L.Z. designed the study, analyzed the results, and wrote the manuscript. N.Y., A.B. and S.G. performed experiments and data analysis. L.Z. helped with the microfluidic assay and flow cytometry experiments. D.S., K.H., and Z.Y. helped recruit iTTP patients. All authors approved the final version of the manuscript for submission.

Non-author contributions and disclosures: No;

Agreement to Share Publication-Related Data and Data Sharing Statement: All raw data will be shared upon request through corresponding author.

Clinical trial registration information (if any):

Targeting Neutrophil Extracellular Trap Accumulation under Flow in Patients with Immune-Mediated Thrombotic Thrombocytopenic Purpura

Short title: ADAMTS13 or Caplacizumab Prevents NET Accumulation in iTTP.

Noritaka Yada[1], Quan Zhang[1], Antonia Bignotti[1], Sarah H. Gralnek[1], Dennis Sosnovske[1], Keenan Hogan[1], Zhan Ye[1], Liang Zheng[1,2], and X. Long Zheng[1,2]†

[1]Department of Pathology and Laboratory Medicine and [2]Institute of Reproductive Medicine and Developmental Sciences, The University of Kansas Medical Center, Kanas City, Kansas 66160

†Correspondence should be sent to:

X. Long Zheng, MD, PhD

Department of Pathology and Laboratory Medicine

The University of Kansas Medical Center

5016 Delp, Mail Stop 3045

3901 Rainbow Blvd,

Kansas City, KS 66160

All raw data will be shared upon request through corresponding author.

Word count: Abstract 249, Text 4,382, Figures x7, Tables x1, Suppl. Table x1, Suppl. Figure x3, Suppl. Videos x10, and References 77.

Key points

- Dynamic changes in neutrophil NETosis in patients with immune-mediated thrombotic thrombocytopenic purpura (iTTP) are assessed.
- Like DNase I, recombinant ADAMTS13 or caplacizumab prevents the accumulation of neutrophil extracellular traps under flow in iTTP.

Summary

Neutrophil NETosis is a unique form of cell death, characterized by release of decondensed chromatin and anti-microbial contents to the extracellular space, involved in infection, inflammation, and thrombosis. However, the role of NETosis in pathogenesis of immune-mediated thrombotic thrombocytopenic purpura (iTTP) and how a targeted therapy affects the accumulation of neutrophil extracellular traps (NETs) under flow remain to be determined. Flow cytometry demonstrated that the percentage of neutrophils undergoing NETosis in whole blood from iTTP patients on admission is significantly increased with a concurrent decrease in the capacity of inducible NETosis by shigatoxin. Following therapy, the percentage of H3Cit+MPO+ neutrophils was significantly reduced with an improvement of inducible NETosis in these patients. Additionally, little to no NET and thrombus formation was detected under flow in whole blood from iTTP patients when platelet counts were very low, but the NET and thrombus formation were dramatically increased following therapy when platelet count rose to $\geq 50 \times 10^9$/L or was restored to normal with donor platelets. Similarly, there was no thrombus and NET accumulation under flow in whole blood from *vwf*$^{-/-}$ mice, but NET accumulation was significantly higher in *Adamts13*$^{-/-}$ than wild-type mice. Finally, recombinant ADAMTS13 or caplacizumab (or anfibatide) prevents the NET and thrombus formation under flow in whole blood from iTTP patients (or *Adamts13*$^{-/-}$ mice). These results indicate that neutrophil NETosis and NET formation depend on platelets and VWF in iTTP, and a targeted therapy such as recombinant ADAMTS13 or caplacizumab may prevent the NET and thrombus formation under flow in iTTP.

Introduction

Immune-mediated thrombotic thrombocytopenic purpura (iTTP) is a rare but potentially fatal hematological disease. It is primarily caused by autoantibody-mediated inhibition of plasma ADAMTS13 activity[1-3] and/or an accelerated clearance of plasma ADAMTS13 antigen[4], resulting in severe deficiency of ADAMTS13 activity. ADAMTS13, primarily synthesized in hepatic stellate cells[5,6] and endothelial cells[7,8], is the key enzyme in circulation to cleave endothelium-derived ultra large von Willebrand factor (VWF) multimers[9]. This proteolytic cleavage of VWF is crucial in maintaining normal hemostasis[10]. Severe deficiency of plasma ADAMTS13 activity results in an accumulation of ultra large VWF multimers on vascular endothelial surfaces, in circulation, and at sites of vascular injury. This leads to excessive platelet aggregation and thrombus formation in small arterioles and capillaries, a characteristic pathological feature of iTTP[11]. Patients with iTTP may present with a marked thrombocytopenia, microangiopathic hemolytic anemia, and various degrees of end organ damage[12-14]. Therapeutic plasma exchange (TPE), caplacizumab, and immunosuppressants (e.g., corticosteroids and rituximab), known as triple therapy, are the standard of care for treatment of iTTP[15,16], while plasma infusion[17,18] or recombinant ADAMTS13[19] appears to be effective for the treatment of hereditary thrombotic thrombocytopenic purpura (hTTP), which results from mutations in *ADAMTS13*, leading to severe deficiency of plasma ADAMTS13 activity.

Surprisingly, severe deficiency of plasma ADAMTS13 alone may not be sufficient to cause an acute episode of iTTP or hTTP, as demonstrated in human[20] and mice[21]. This suggests that additional environmental or genetic factors such as infections or acute systemic inflammation may be required to trigger acute TTP. *Adamts13*$^{-/-}$ mice

do not develop spontaneous thrombocytopenia unless being challenged with a bacterial toxin such as shigatoxin-2 or a large dose of unprocessed recombinant VWF[21-23]. Shigatoxin-2 has been shown to activate endothelium to release ultra large VWF, result in endothelial injury[21,22,24], and trigger neutrophils NETosis[25], all of which may lead to microvascular thrombosis when plasma ADAMTS13 activity is severely deficient. *Adamts13*$^{-/-}$ mice carrying a loss-functional heterozygous mutation (W1206R) in complement factor H (*cfh*) also developed spontaneous thrombotic microangiopathy while a loss of function in either *Adamts13* or *cfh* was not sufficient to cause the disease[26].

NETosis is part of the innate immune system used for self-defense. It protects host from invasion by an external agent such as bacteria, fungi, and virues[27,28]. Neutrophil NETosis may play a role in pathogenesis of various inflammatory diseases, including sepsis[29,30], systemic lupus erythematosus,[31] and thrombotic diseases (e.g., deep vein thrombosis, heparin-induced thrombocytopenia[30,32], and acute iTTP[33-35]. However, the dynamic change of neutrophil NETosis and the ability to form NETs under flow in iTTP patients or *Adamts13*$^{-/-}$ mice have not been extensively studied. Additionally, the effect of current targeted therapy for iTTP such as recombinant ADAMTS13 or caplacizumab on the NET accumulation under flow has not been investigated. Thus, the present study aims to determine the extent of neutrophil NETosis *in vivo* and inducible NETosis by an external agonist in acute iTTP and during treatment, and assess the role of platelets, VWF, and ADAMTS13, as well as a targeted therapeutic for iTTP on the NET accumulation under arterial flow.

Methods

Patients: Institutional Review Board (IRB) at the University of Kansas Medical Center

approved the study protocol (#STUDY00145731). Consecutive patients at the University of Kansas Hospital between June 2022 and June 2023 with a suspected iTTP were prospectively enrolled into the study. Diagnosis of iTTP was made on the following criteria: thrombocytopenia and microangiopathic hemolytic anemia with organ damage[36]. All patients were subsequently confirmed to have a plasma ADAMTS13 activity level <10 IU/dL and a positive anti-ADAMTS13 IgG (**Table S1**). One patient whose first sample was collected more than 48 hours after admission was excluded to avoid the impact of therapeutic plasma exchange (TPE) on the assessment of plasma ADAMTS13 activity, inhibitor, and neutrophil NETosis. Samples from those without an acute iTTP and other hematological diseases were obtained for the controls. All patients participated in the study were informed and consented.

Samples and clinical data: Venous blood samples were collected from non-TTP controls and patients admitted for acute iTTP patients prior to and during therapy. The whole blood was anti-coagulated with ethylenediaminetetraacetic acid (EDTA) for flow cytometric analysis or 3.2% sodium citrate for shear-based assay. Patient demographic information, clinical characteristics, and laboratory data were collected from electronic medical records. Laboratory findings include white blood cell count, neutrophil count, hemoglobin level, hematocrit, platelet count, lactate dehydrogenase (LDH) level, prothrombin time, activated partial thromboplastin time, creatinine level, ADAMTS13 activity, and anti-ADAMTS13 IgG levels.

Murine model of TTP. All animal experimental protocols were approved by the Institutional Animal Care and Use Committee (ACUP #2020-2574) of the University of Kansas Medical Center. *Adamts13*$^{-/-}$ mice in the CAST/Ei strain were used in

these studies[21]. Murine whole blood was collected via a retro-orbital bleeding technique following anesthesia. Approximately 70 µL of whole blood was collected and anticoagulated with a thrombin inhibitor D-Phenylalanyl-L-prolyl-L-arginine chloromethyl ketone (PPACK) (100 µmol/L). The whole blood was treated *ex vivo* with 100 ng/mL of Stx-2 for 60 min[25] prior to perfusion through the microchannels coated with type 1 fibrillar collagen from equine tendons (Crono-log, Havertown, PA) under 100 dyne/cm^2 for 120 seconds[37].

Critical reagents. Recombinant ADAMTS13 was expressed in stably transfected HEK-293 cells using 10-layer cell factories (ThermoFisher, Waltham, MA) in serum-free DMEM/F12 medium supplemented with 1% of insulin, transferrin, and selenium (ITS) cocktail (Millipore-Sigma, Burlington, MA)[38,39]. Approximately 2L of conditioned medium was collected daily and loaded onto a Q-fast flow ion exchange (Thermo Fisher) column. Total proteins were eluted with 1.0 M NaCl in 20 mM Tris-HCl, pH 8.0. All fractions containing proteins were pooled and then loaded onto a 10-80 mL Ni-NTA affinity column (ThermoFisher). After being washed with 20 mM and 40 mM of imidazole, the bound proteins were eluted with 250 mM of imidazole in 20 mM Tris-HCl, pH 8.0, and 400 mM NaCl. The peak fractions containing recombinant ADAMTS13 protein were pooled and concentrated with a Centri-Prep30 (Millipore, Billerica, MA) and buffer-exchanged with 10 mM HEPES, pH 7.4, containing 150 mM NaCl and 5 mM $CaCl_2$. This essentially removes imidazole and recharges rADAMTS13 with appropriate divalent metal ions. The SDS–polyacrylamide gel electrophoresis (PAGE) with Coomassie blue staining and the absorbance at 280nm determined the purity and concentration of recombinant ADAMTS13, respectively.

Flow cytometry. Whole blood anticoagulated with EDTA was centrifuged at 500xg for

10 minutes to obtain a buffy coat, which was washed with phosphate-buffered saline (PBS) containing 2% bovine serum albumin[40]. It was then incubated with 100 ng/mL of Stx-2 (Toxin Technology, Sarasota, FL) for 15 minutes to stimulate neutrophil NETosis[25]. The cells were fixed with 2% paraformaldehyde for 30 minutes and the neutrophils were identified with eFluor450 anti-CD15 (Invitrogen). Citrullinated histone H3 (H3Cit) was stained with anti-citrullinated histone H3 (citrulline at R2, R8, and R17) IgG (Abcam, Waltham, MA), followed by a goat Alexa488-conjugated anti-rabbit IgG (ThermoFisher). Myeloperoxidase (MPO) in neutrophils was stained with PE anti-MPO antibody (Novus Biologicals, Centennial, CO) as previously described[29,30,32,41]. The stained cells were analyzed by BD LSR II flow cytometer.

Assay for plasma myeloperoxidase levels. Plasma levels of myeloperoxidase (MPO) were determined using an ELISA kit [34] from ThermoFisher according to manufacturer's recommendation.

ADAMTS13 activity and antibody in patients with iTTP. Plasma ADAMTS13 activity and anti-ADAMTS13 IgG were determined using the Technozym ADAMTS13 activity and antibody Kit (DiaPharma, West Chester, OH) as previously described[42]. The lowest detection limit for plasma ADAMTS13 activity is 0.1%. Plasma level of anti-ADAMTS13 IgG greater than 15 U/mL is interpreted positive.

Microfluidic shear-based assay. Patient whole blood anticoagulated with sodium citrate was stained with rhodamine 6G (Sigma-Aldrich, St. Louis, MO) at 40 µg/mL for 15 min. The whole blood was then perfused at 100 dyne/cm^2 over micro channels coated with type 1 fibrillar collagen (100 µg/mL) (Chrono-Log, Overland Park, KS) in 0.01M HCl and blocked with PBS/ 0.5% BSA[37]. One of the channels was perfused with a whole blood aliquot pre-incubated with DNase I (or pulmozyme) (200 U/mL)

(Genentech, San Francisco, CA), recombinant ADAMTS13 (6 μg/mL) or caplacizumab (3 μg/mL) (Sanofi, Chattanooga, TN) for 15 min. Additionally, *Adamts13*$^{-/-}$ mouse blood anti-coagulated with 100 μmol/L of PPACK (Sigma- Aldrich, St. Louis, MO) in the presence of 3 μmol/L of prostaglandin E1 (Sigma-Aldrich) was treated with 100 ng/mL of Stx-2 in a CO_2 incubator at 37°C for 1 hour to trigger NETosis and diluted 2-fold with Tyrode's buffer (10 mmol/L HEPES, pH 7.4, 134 mmol/L NaCl, 2.7 mmol/L KCl, 1.0 mmol/L $MgCl_2$, 12 mmol/L $NaHCO_3$, and 0.34 mmol/L Na_2HPO_4) prior to perfusion in the absence or presence of DNase I, recombinant ADAMTS13, or anfibatide (1.5 μg/mL). The rate of thrombus formation (or the rate of platelet and neutrophil accumulation) was recorded every 3 seconds for 120 seconds[37]. The surface area coverage was determined with Montage software. At the completion of the real time experiment, the cells in the micro channels were fixed with 4% paraformaldehyde and stained with SytoxGreen (0.3 μmol/L) (ThermoFisher), nuclei with Hoechst 33342 (10 μg/mL) (ThermoFisher), and platelets with anti-human CD41 (BD Biosciences, Lakes, NJ) or anti-mouse CD41 (5 μg/mL) conjugated with APC (Biolegend, San Diego, CA). The fluorescent images were obtained under a Nikon A1R confocal microscope using the NIS- Elements Viewer 5.21 (Melville, NY).

Ex vivo restoration of thrombocytopenia in iTTP patient with donor platelets. Platelet-rich plasma was prepared following a centrifugation of donor blood anti-coagulated with sodium citrate at 150xg for 15 minutes. A Tyrode's buffer was added to platelet-rich plasma, followed by centrifugation at 900xg for 10 minutes to obtain platelet pellets[37]. These platelet pellets were resuspended in Tyrode's buffer prior to use for the restoration of thrombocytopenia in the whole blood of iTTP patients.

Cleavage of VWF by ADAMTS13 and DNase I under shear. Plasma-derived VWF (8.3 μg/mL) was incubated with recombinant ADAMTS13 (30 μg/mL) or DNase I (200 U/mL) in the absence or presence of EDTA for 30 min under constant vortexing at 2,500 rpm in a PCR mixer. Sample buffer was added to the PCR tube and heated at 100 °C for 5 min to terminate the reaction. The denatured proteins were separated with 1% agarose gel electrophoresis. The VWF multimer distribution was determined by Western blotting with anti-VWF IgG, followed by IRDye800 anti-rabbit IgG (LI-COR, Lincoln, Nebraska) as described previously[43].

Statistical Analysis. Mann-Whitney tests and Kruskal-Wallis ANOVA tests were used for non-parametric data of two groups and greater than three groups, respectively. Paired *t*-tests were used for changes in the same groups for normally distributed data, but Wilcoxon signed-rank tests were used for non-parametric data. Statistical significance was set at $p<0.05$. Data analysis and graphing were performed using Prism 9 software (GraphPad, Boston, MA).

Results

Patient characteristics. All six patients enrolled into the study had clinical and laboratory characteristics that were consistent with the diagnosis of iTTP according to 2020 ISTH guidelines[36]. The mean (± SD) age was 53.8 (±13.8) years with an equal gender distribution. Hypertension and chronic renal disease were found in 2/6 (33.3%) of cases. The mean (± SD) platelet count was 9.7 (± 4.8) $x10^9$/L. All patients had plasma ADAMTS13 activity levels less than 1.0 IU/dL (or 1% of normal) and positive anti-ADAMTS13 antibodies. Hemoglobin and hematocrit (mean ± SD) were 9.4 ± 3.9 g/dL and 27.0 ± 11.6%, respectively. Lactate dehydrogenase and creatinine were 1,444 ± 836 IU/L and 1.7 ± 1.1 mg/dL, respectively, with normal prothrombin

time (PT) and activated thromboplastin time (APTT) (**Table 1**). All patients were treated with TPE daily, corticosteroids, and upfront rituximab. Five patients also received caplacizumab with 3-4 days of admission. One patient case was complicated by intracranial bleeding and did not receive caplacizumab (**Table S1**).

NETosis and its potential of inducible NETosis in patients with acute iTTP. Using flow cytometry, we were able to detect a small percentage (median, 2.1%) of neutrophils undergoing NETosis, marked by H3Cit+MPO+, in whole blood from non-TTP controls (**Fig. 1A**). The median percentage of the H3Cit+ and MPO+ neutrophils in patients with acute iTTP was 11.3% (**Fig. 1B**), significantly higher than that in non-TTP controls. Following a standard of care therapy, the median percentage of H3Cit+ and MPO+ neutrophil was significantly reduced (to 0.9%) (**Fig. 1C**). The difference in the percentage of H3Cit+ and MPO+ neutrophils was statistically significant between the control and iTTP patients on admission (p<0.05) or between iTTP patients on admission and iTTP patients during clinical remission (p<0.05) (**Fig. 1G**). Plasma levels of MPO in iTTP patients on admission were significantly higher than those during clinical response/remission (p<0.05) **(Fig. 1H).** These results indicate that neutrophil NETosis is significantly elevated in acute iTTP, which is markedly reduced following a standard of care therapy or during remission.

To assess the NETosis reserve (or the potential of inducible NETosis), shigatoxin-2 (Stx-2) that was shown to induce thrombotic microangiopathy in humans[44] and in mice[21,45,46] was used to trigger neutrophil NETosis. A whole blood sample was incubated with Stx-2 (100 ng/mL) at 37 °C for 15 min prior to fixation, staining, and flow cytometric analysis. The results showed that following Stx-2 stimulation the percentage of neutrophils with H3Cit+MPO+ staining was increased by 2.6-fold (from

2.2% to 5.7%) (p<0.01) (**Fig. 1D**), but much less so in iTTP on admission (from 11.3% to 12.2%, (p>0.05) (**Fig. 1E**). The percentage was significantly increased again in iTTP during clinical response/remission (from 0.9% to 6.1%, 6..8-fold increase (p<0.05) (**Fig. 1F**). Quantitative data and statistical analysis of the percentage of NETosis prior to and after Stx-2 challenge are shown (**Fig. 1I, 1J, and 1K)**. These results indicate that neutrophil NETosis reserve may be significantly reduced in acute iTTP, which recovers following an intensive therapy.

Thrombus and NET accumulation on collagen surface under flow in WT, vwf$^{-/-}$, and Adamts13$^{-/-}$ mice. To determine if VWF and ADAMTS13 regulate the shear-dependent accumulation of NETs, we collected PPACK-anticoagulated whole blood samples from wild type (*WT*), *vwf*$^{-/-}$, and *Adamts13*$^{-/-}$ mice (CAST/Ei strain) and challenged with Stx-2 (100 ng/mL) at 37°C for 1 hour to induce neutrophil NETosis. Without Stx-2 stimulation, no NET was detected despite many platelets and neutrophils adhered to the collagen surface under flow (Fig. S2). Following perfusion of Stx-2-stimulated whole blood, the rate of thrombus formation under flow was significantly lower in *vwf*$^{-/-}$ mice than the *WT* controls (**Fig. 2A**, **2B,** Video **S1**) as expected. Conversely, the rate of thrombus formation following perfusion of stimulated blood from *Adamts13*$^{-/-}$ mice was much higher than that in *WT* controls (**Fig. 2C, 2D,** Video **S2**). Interestingly, the NET accumulation was also significantly reduced following perfusion of whole blood from the *vwf*$^{-/-}$ mice (**Fig. 2E/E'**) but increased in that from *Adamts13*$^{-/-}$ mice (**Fig. 2F/F'**) when compared with that from *WT* mice. The number of elongated DNA strings under a florescent microscope following perfusion of a whole blood from *WT*, *vwf*$^{-/-}$, and *Adamts13*$^{-/-}$ mice was statistically significantly different (**Fig. 2G)**. Together, these results indicate that like thrombus formation the neutrophil NETosis and NET accumulation under flow

depends on plasma VWF, which is regulated by ADAMTS13 proteolysis.

Recombinant ADAMTS13 and anfibatide inhibit thrombus formation and NET accumulation on collagen surface under flow in Adamts13$^{-/-}$ mice. To determine if a targeted therapy, ADAMTS13 that cleaves VWF or anfibatide that inhibits VWF-platelet interaction, inhibits NET accumulation under flow, we perfused a PPACK-anticoagulated whole blood from *Adamts13$^{-/-}$* mice stimulated with Stx-2 over a type I fibrillar collagen surface under 100 dyne/cm^2 in the absence or presence of recombinant human ADAMTS13 or anfibatide. The results showed that the rate of thrombus formation was significantly reduced in the channels where DNase I (**Fig. 3A, 3D,** Video **S3**) or recombinant ADAMTS13 (**Fig. 3B/3E,** Video **S4**), or anfibatide (**Fig. 3C, 3F,** Video **S5**) was present, compared with that in the channel where DNase I, recombinant ADAMTS13 or anfibatide was absent. More interestingly, the characteristic, elongated, and extracellularly stained DNA strings (NETs) were found only in the channels in the absence of DNase I, or recombinant ADAMTS13, or anfibatide present (**Figs. 3G/G', 3H/H',** and **3I/I'**). The number of DNA strings under microscope with or without DNase I was statistically significantly different (**Figs. 3J, 3K,** and **3L**). These results indicate that neutrophils NETosis induced by shigatoxin in a whole blood from *Adamts13$^{-/-}$* mice is significantly enhanced, which could be removed by DNase I, or prevented by recombinant human ADAMTS13 or anfibatide.

Recombinant ADAMTS13 and caplacizumab inhibit thrombus formation and NET accumulation on collagen surface under flow in iTTP. To assess the dynamic change of thrombus formation and NET accumulation under flow, and the therapeutic effect of DNase I, recombinant ADAMTS13, and caplacizumab on eliminating or preventing thrombus formation and NET accumulation, we collected citrated-anticoagulated

whole blood samples from 6 patients with acute iTTP on admission when platelet count was very low (<10x10^9/L) and during clinical responses/remission (5 cases) or when platelet counts rose to >30x10^9/L (1 case) (**Table S1)**. The anticoagulated whole blood was then perfused over a type I fibrillar collagen coated surface at 100 dyne/cm^2 in the absence or presence of DNase I, or recombinant ADAMTS13, or caplacizumab. As expected, no platelet or neutrophil adhered to the collagen surface when a whole blood (very low platelet count) from acute iTTP on admission was perfused (**Fig. 4A, 4C,** Video **S6**). At the same time, little or no NET was observed on the collagen surface following SytoxGreen staining (**Fig. 4E/E'**). However, when donor platelets were added to these initial iTTP patient samples to normalize platelet counts, both thrombus formation and NET accumulation on the collagen surface were dramatically increased under the same flow conditions, which could be abrogated by caplacizumab (**Fig. S3** and Video **S7**). Moreover, the thrombus formation (**Fig. 4B, 4D,** Video **S8**) and NET accumulation (**Fig. 4F/F'**) were also significantly increased in the iTTP patient samples following the standard of care therapy when platelet counts were normalized or substantially increased, despite being treated with TPE and/or caplacizumab. Quantitation of the number of elongated DNA strings in the absence or presence of DNase I demonstrated the significant difference in patient samples collected after therapy (**Fig. 4F**, **4H)**. These results demonstrate that platelets may play a role in NET accumulation onto collagen surface under flow in patients with acute iTTP, which can be completely removed by DNase I.

To further determine if recombinant ADAMTS13 is efficacious in preventing NET accumulation on collagen surface under flow, we perfused an anticoagulated whole blood from iTTP patients in the presence or absence of recombinant human

ADAMTS13 (6 μg/mL) or caplacizumab (3 μg/mL) over the collagen-coated surface. Consistently, the rate of thrombus formation on the collagen surface were very low in iTTP patient blood samples collected on admission when platelet counts were very low despite severe ADAMTS13 deficiency (**Fig. 5A, 5C** or **Fig**. **6A, 6C**); the thrombus formation was dramatically increased in patient samples obtained from iTTP patients after therapy when platelet counts were normalized or substantially increased but plasma ADAMTS13 activity remained quite low (**Fig. 5B, 5D** or **Fig. 6B, 6D**). Similarly, the NETs formed on the collagen surface were also extremely low in the patient admission blood samples (**Fig. 5E/E'** and **5G** or **Fig. 6E/E'** and **6G**) but dramatically increased in the samples during clinical remission when platelet counts were normalized or substantially increased (**Fig. 5F/F'** and **5H** or **Fig. 6F/F'** and **6H**). Interestingly, the addition of either recombinant ADAMTS13 (**Fig. 5,** Video **S9**) or caplacizumab (3 μg/mL) (**Fig. 6** and Video **S10**) further reduced thrombus formation and NET accumulation on the collagen surface in all blood samples. Together, our results demonstrate that the thrombus formation and NET accumulation under flow in whole blood from patients depends on platelet counts and VWF function. Like DNase I, recombinant ADAMTS13 and caplacizumab may prevent thrombus formation and NET accumulation under flow in iTTP.

DNase I does not cleave VWF under flow. To determine if DNase I cleaves VWF, we incubated a purified plasma VWF with a high concentration of DNase I (200 U/mL) or recombinant ADAMTS13 (30 μg/mL) for 30 min under constant shear. Based on agarose gel electrophoresis and Western blotting analysis of VWF multimer distribution, we found that DNase I at the concentration used in the microfluidic assays did not cleave VWF multimers directly, while recombinant ADAMTS13 did as expected. The cleavage of VWF by ADAMTS13 was completely inhibited by the

addition of EDTA (20 mM), suggesting the cleavage of VWF is specific for a metalloprotease ADAMTS13 (**Fig. S1**).

Discussion

To our knowledge this is the first demonstration of the dynamic changes of neutrophil NETosis, NETosis reserve, thrombus formation, and NET accumulation in acute iTTP. More importantly, we demonstrate that, like DNase I, recombinant ADAMTS13 or caplacizumab (or anfibatide) prevents the NET accumulation in iTTP under flow through proteolytic cleavage of VWF or inhibition of VWF-platelet interaction, providing novel insight into the mechanism how recombinant ADAMTS13 or anti-VWF nanobody may function as an anti-thrombotic and anti-inflammatory agent.

iTTP is primarily caused by autoantibodies against ADAMTS13, resulting in severe deficiency of plasma ADAMTS13 activity[1-3]. However, plasma ADAMTS13 deficiency alone may not be sufficient to cause an acute episode of TTP, suggesting that a second trigger may be necessary. Pregnancy, infection, and inflammation are the most common physiological or environmental factors that trigger acute iTTP[47-49]. This is because pregnancy may activate the complement system and induce a hypercoagulable state, including an increased expression of VWF and other coagulation factors but a reduced activity of anticoagulants such as ADAMTS13, protein C, protein S, tissue plasminogen inhibitors (PAI-1), etc.[50,51]. During pregnancy, the balance between pro-inflammatory Th2 cytokines (e.g., interferon-γ and tumor necrosis factor-α) and anti-inflammatory Th2 cytokines (e.g., interleukin-10) is fundamental for successful gestation[52-54].

Inflammation may trigger neutrophils to undergo NETosis, resulting in release of

NETs[55]. NETosis is an innate immune response, which helps localize infection and serves as a scaffold for the development of platelet-rich thrombi[56-58]. The formation of NETs requires VWF and platelets and together they serve as a platform for neutrophil rolling interaction and adherence[59-61]. NETs are rapidly degraded by DNase I, whose activity is significantly decreased in patients with acute iTTP[62] and other pathological conditions such as COVID-19[63,64] and lupus[65,66]. Excessive NETs may result in vascular endothelial injury and subsequent organ damage[67,68].

Elevated plasma levels of soluble NETs fragments (i.e., histone-DNA or histone-MPO complexes) or cell-free DNA in patients with acute iTTP are reported[33,34]. The increased levels of NETs are associated with the disease severity and mortality rate of iTTP[33]. Several previous studies have also used flow cytometry to assess the NETosis in patients with sepsis, systemic lupus erythematous, deep vein thrombosis, and heparin-induced thrombocytopenia[29-32,69]. Phorbol myristate acetate (PMA), bacteria, and viruses are known to stimulate NET formation[70-72] and the changes following a stimulation with PMA are much less pronounced in septic patients than in healthy controls, suggesting the reduced NETosis reserve in these patients[30]. In our study, we show that Stx-2, implicated in the development of HUS, does not further stimulate NETosis in the admission blood from acute iTTP, but does increase NETosis in the blood samples from patients after therapy. These results indicate that the number of neutrophils capable of undergoing NETosis (or NETosis reserve) in acute iTTP may be significantly reduced due to massive NETosis and a NETosis reserve can be restored in iTTP following a standard of care therapy.

The therapeutic efficacy of DNase I that eliminates NETs has been previously tested in a murine model of acute respiratory distress syndrome[73] and in patients with acute

COVID-19[64]. DNase I does not directly cleave VWF multimers under shear but does digest the extracellular DNA strings, thus reducing inflammation and thrombosis.

To assess if NET formation or accumulation under flow can be prevented by cleaving VWF or inhibiting VWF-platelet interaction, we performed microfluidic assays. Our results demonstrate that there are no thrombi or NET accumulation on collagen surface under flow in iTTP on admission when platelet count is extremely low ($<10x10^9$/L). Both thrombus formation and NET accumulation under flow increase dramatically following a reconstitution of platelet counts using donor platelets or after platelet counts rise following therapy. This supports that both thrombus formation and NET accumulation are dependent on platelets, which are required for neutrophils to adhere to the VWF-collagen surface via CD62[74]. This hypothesis is further supported by demonstrating that the disruption of platelet-VWF interaction with recombinant ADAMTS13 that cleaves VWF or caplacizumab that binds the A1 domain of VWF[75,76] or anfibatide that binds platelet GPIb[46,77] inhibits thrombus formation and NET accumulation under flow in both iTTP patient and *Adamts13*$^{-/-}$ murine whole blood perfused over collagen-coated surface under flow.

There are some limitations in this study. While flow cytometry is widely used for assessing neutrophil NETosis in vivo, the stability and structural accessibility of CitrH3 and MPO on activated neutrophils may create variability in quantitation. Therapeutic intervention such as plasma exchange and caplacizumab may affect the levels of soluble NETs in plasma. Finally, the number of acute iTTP cases studied for NETosis *in vivo* and NET accumulation under flow remains to be small. Nevertheless, these limitations do not affect our interpretation and conclusion of the study.

We conclude that neutrophil NETosis is significantly elevated and its NETosis reserve is significantly reduced in acute iTTP. Both return to normal following a standard of care therapy. Little or no thrombus formation and NET accumulation under flow were observed in iTTP on admission when platelet count is very low, but they are significantly increased following therapy when platelet counts are substantially increased or normalized. Most importantly, like DNase I, recombinant ADAMTS13 or caplacizumab (or anfibatide) prevents the accumulation of NETs on collagen surface under flow, likely via inhibition of VWF function or disruption of VWF-platelet-neutrophil interaction. Together, our findings support a potential contribution of NETosis and NET formation in pathogenesis of iTTP and reveal an additional mechanism underlying the anti-inflammatory and anti-thrombotic effects of recombinant ADAMTS13 or caplacizumab (or anfibatide) as a targeted therapy for iTTP and perhaps other inflammatory and thrombotic disorders.

Authors' contributions

N.Y. Q.Z., and X.L.Z. designed the study, analyzed the results, and wrote the manuscript. N.Y., A.B. and S.G. performed experiments and data analysis. L.Z. helped with the microfluidic assay and flow cytometry experiments. D.S., K.H., and Z.Y. helped recruit iTTP patients. All authors approved the final version of the manuscript for submission.

Acknowledgements

The study was supported in part by grants from NHLBI (HL144552, HL157975-01A1, and HL164016-01A1) and Answering T.T.P. Foundation to X.L.Z. Authors express our gratitude toward Ms. Lucy Zheng for her assistance in designing graphic abstract and subtitle labeling using iMovie.

Disclosure

X.L.Z. is a consultant for Alexion, Apollo, GC Biopharma, Sanofi, Stago, and Takeda. X.L.Z. is also the co-founder of Clotsolution. All other authors have declared no relevant conflict.

Table 1. Characteristics and Laboratory findings on admission of six iTTP patients used in the microfluidic assays.

Parameter	Reference#	iTTP (n=6)
Age (years)	-	53.8 ± 13.8*
Gender, male, n (%)	-	3 (50.0)
Comorbidities		
- Hypertension, n (%)	-	2 (33.3)
- Diabetes, n (%)	-	0 (0)
- Chronic kidney disease, n (%)	-	2 (33.3)
- History of malignancy, n (%)	-	2 (33.3)
White Blood Cell ($x10^9$/L)	4.5-11.0	10.7 ± 3.0*
Neutrophil ($x10^9$/L)	4.1-7.7	8.5 ± 2.3*
Hemoglobin (g/dL)	12.0-16.5	9.4 ± 3.9*
Hematocrit (%)	36-50	27.0 ± 11.6*
Platelet count ($x10^9$/L)	150-400	9.7 ± 4.8*
ADAMTS13 activity (IU/dL) Anti-ADAMTS13 IgG (U/mL)	40-133 <15	0 (0-0.7)** Positive
LDH (IU/L)	100-200	1444 ± 836*
Creatinine (mg/dL)	0.46-1.09	1.7 ± 1.1*
INR	0.85-1.15	1.2 ± 0.2*
APTT (sec)	20-40	29.0 ± 2.1*

*Data are shown as the mean ± standard deviation (SD); **median (range); LDH, lactate dehydrogenase; INR, international normalized ratio; APTT, activated thromboplastin time. #Laboratory reference ranges are provided.

References

1. Furlan M, Robles R, Solenthaler M, Lammle B. Acquired deficiency of von Willebrand factor-cleaving protease in a patient with thrombotic thrombocytopenic purpura. *Blood*. 1998;91(8):2839-2846.

2. Tsai HM, Lian EC. Antibodies to von Willebrand factor-cleaving protease in acute thrombotic thrombocytopenic purpura. *N Eng J Med*. 1998;339(22):1585-1594.

3. Zheng XL, Wu HM, Shang D, et al. Multiple domains of ADAMTS13 are targeted by autoantibodies against ADAMTS13 in patients with acquired idiopathic thrombotic thrombocytopenic purpura. *Haematologica*. 2010;95(9):1555-1562.

4. Underwood MI, Alwan F, Thomas MR, Scully MA, Crawley JTB. Autoantibodies enhance ADAMTS-13 clearance in patients with immune thrombotic thrombocytopenic purpura. *J Thromb Haemost*. 2023;21(6):1544-1552.

5. Uemura M, Tatsumi K, Matsumoto M, et al. Localization of ADAMTS13 to the stellate cells of human liver. *Blood*. 2005;106(3):922-924.

6. Zhou W, Inada M, Lee TP, et al. ADAMTS13 is expressed in hepatic stellate cells. *Lab Invest*. 2005;85(6):780-788.

7. Shang D, Zheng XW, Niiya M, Zheng XL. Apical sorting of ADAMTS13 in vascular endothelial cells and Madin-Darby canine kidney cells depends on the CUB domains and their association with lipid rafts. *Blood*. 2006;108(7):2207-2215.

8. Kling SJ, Judd CA, Warner KB, Rodgers GM. Regulation of ADAMTS13 expression in proliferating human umbilical vein endothelial cells. *Pathophysiol Haemost Thromb*. 2008;36(5):233-240.

9. Dong JF, Moake JL, Nolasco L, et al. ADAMTS-13 rapidly cleaves newly secreted ultralarge von Willebrand factor multimers on the endothelial surface under flowing conditions. *Blood*. 2002;100(12):4033-4039.

10. Sadler JE. A new name in thrombosis, ADAMTS13. *Proc Natl Acad Sci U S A*. 2002;99(18):11552-11554.

11. Zheng XL. ADAMTS13 and von Willebrand factor in thrombotic thrombocytopenic purpura. *Annu Rev Med*. 2015;66:211-225.

12. Bell WR, Braine HG, Ness PM, Kickler TS. Improved survival in thrombotic thrombocytopenic purpura-hemolytic uremic syndrome. Clinical experience in 108 patients. *N Engl J Med*. 1991;325(6):398-403.

13. Furlan M, Lammle B. Deficiency of von Willebrand factor-cleaving protease in familial and acquired thrombotic thrombocytopenic purpura. *Bailliere's clinical haematology*. 1998;11(2):509-514.

14. Zheng XL, Kaufman RM, Goodnough LT, Sadler JE. Effect of plasma exchange on plasma ADAMTS13 metalloprotease activity, inhibitor level, and clinical outcome in patients with idiopathic and nonidiopathic thrombotic thrombocytopenic purpura. *Blood*. 2004;103(11):4043-4049.

15. Zheng XL, Vesely SK, Cataland SR, et al. ISTH guidelines for treatment of thrombotic thrombocytopenic purpura. *J Thromb Haemost*. 2020;18(10):2496-2502.

16. Zheng XL. The standard of care for immune thrombotic thrombocytopenic purpura today. *J Thromb Haemost*. 2021.

17. Fujimura Y, Matsumoto M, Yagi H, Yoshioka A, Matsui T, Titani K. Von Willebrand factor-cleaving protease and Upshaw-Schulman syndrome. *Int J Hematol*. 2002;75(1):25-34.

18. Fujimura Y, Matsumoto M. Registry of 919 patients with thrombotic microangiopathies across Japan: database of Nara Medical University during 1998-2008. *Intern Med*. 2010;49(1):7-15.

19. Scully M, Knobl P, Kentouche K, et al. Recombinant ADAMTS-13: first-in-human pharmacokinetics and safety in congenital thrombotic thrombocytopenic purpura. *Blood*. 2017;130(19):2055-2063.

20. Fujimura Y, Matsumoto M, Isonishi A, et al. Natural history of Upshaw-Schulman syndrome based on ADAMTS13 gene analysis in Japan. *J Thromb Haemost*. 2011;9 Suppl 1:283-301.

21. Motto DG, Chauhan AK, Zhu G, et al. Shigatoxin triggers thrombotic thrombocytopenic purpura in genetically susceptible ADAMTS13-deficient mice. *J Clin Invest*. 2005;115(10):2752-2761.

22. Huang J, Motto DG, Bundle DR, Sadler JE. Shiga toxin B subunits induce VWF secretion by human endothelial cells and thrombotic microangiopathy in ADAMTS13-deficient mice. *Blood*. 2010;116(18):3653-3659.

23. Jin SY, Xiao J, Bao J, Zhou S, Wright JF, Zheng XL. AAV-mediated expression of an ADAMTS13 variant prevents shigatoxin-induced thrombotic thrombocytopenic purpura. *Blood*. 2013;121(19):3825-3829, S3821-3823.

24. Nolasco LH, Turner NA, Bernardo A, et al. Hemolytic uremic syndrome-associated Shiga toxins promote endothelial-cell secretion and impair ADAMTS13 cleavage of unusually large von Willebrand factor multimers. *Blood*. 2005;106(13):4199-4209.

25. Feitz WJC, Suntharalingham S, Khan M, et al. Shiga Toxin 2a Induces NETosis via NOX-Dependent Pathway. *Biomedicines*. 2021;9(12).

26. Zheng L, Zhang D, Cao W, Song WC, Zheng XL. Synergistic effects of ADAMTS13 deficiency and complement activation in pathogenesis of thrombotic microangiopathy. *Blood*. 2019;134(13):1095-1105.

27. Branzk N, Papayannopoulos V. Molecular mechanisms regulating NETosis in infection and disease. *Semin Immunopathol*. 2013;35(4):513-530.

28. Yildiz K. Netosis: Alternative Defense Method Used by Neutrophils to Fight Pathogen. *Turkiye Parazitol Derg*. 2016;40(3):158-162.

29. Gavillet M, Martinod K, Renella R, et al. Flow cytometric assay for direct quantification of neutrophil extracellular traps in blood samples. *Am J Hematol*. 2015;90(12):1155-1158.

30. Lee KH, Cavanaugh L, Leung H, et al. Quantification of NETs-associated markers by flow cytometry and serum assays in patients with thrombosis and sepsis. *Int J Lab Hematol*. 2018;40(4):392-399.

31. Zharkova O, Tay SH, Lee HY, et al. A Flow Cytometry-Based Assay for High-Throughput Detection and Quantification of Neutrophil Extracellular Traps in Mixed Cell Populations. *Cytometry A*. 2019;95(3):268-278.

32. Perdomo J, Leung HHL, Ahmadi Z, et al. Neutrophil activation and NETosis are the major drivers of thrombosis in heparin-induced thrombocytopenia. *Nat Commun*. 2019;10(1):1322.

33. Sui J, Lu R, Halkidis K, et al. Plasma levels of S100A8/A9, histone/DNA complexes, and cell-free DNA predict adverse outcomes of immune thrombotic thrombocytopenic purpura. *J Thromb Haemost*. 2021;19(2):370-379.

34. Fuchs TA, Kremer Hovinga JA, Schatzberg D, Wagner DD, Lammle B. Circulating DNA and myeloperoxidase indicate disease activity in patients with thrombotic microangiopathies. *Blood*. 2012;120(6):1157-1164.

35. Staley EM, Cao W, Pham HP, et al. Clinical factors and biomarkers predict outcome in patients with immune-mediated thrombotic thrombocytopenic purpura. *Haematologica*. 2019;104(1):166-175.

36. Zheng XL, Vesely SK, Cataland SR, et al. ISTH guidelines for the diagnosis of thrombotic thrombocytopenic purpura. *J Thromb Haemost*. 2020;18(10):2486-2495.

37. Abdelgawwad MS, Cao W, Zheng L, Kocher NK, Williams LA, Zheng XL. Transfusion of Platelets Loaded With Recombinant ADAMTS13 (A Disintegrin and Metalloprotease With Thrombospondin Type 1 Repeats-13) Is Efficacious for Inhibiting Arterial Thrombosis Associated With Thrombotic Thrombocytopenic Purpura. *Arterioscler Thromb Vasc Biol*. 2018;38(11):2731-2743.

38. Ai J, Smith P, Wang S, Zhang P, Zheng XL. The proximal carboxyl-terminal domains of ADAMTS13 determine substrate specificity and are all required for cleavage of von Willebrand factor. *J Biol Chem*. 2005;280(33):29428-29434.

39. Zhang P, Pan W, Rux AH, Sachais BS, Zheng XL. The cooperative activity between the carboxyl-terminal TSP1 repeats and the CUB domains of ADAMTS13 is crucial for recognition of von Willebrand factor under flow. *Blood*. 2007;110(6):1887-1894.

40. Iqbal Z, Absar M, Akhtar T, et al. Integrated Genomic Analysis Identifies ANKRD36 Gene as a Novel and Common Biomarker of Disease Progression in Chronic Myeloid Leukemia. *Biology (Basel)*. 2021;10(11).

41. Mauler M, Seyfert J, Haenel D, et al. Platelet-neutrophil complex formation-a detailed in vitro analysis of murine and human blood samples. *J Leukoc Biol*. 2016;99(5):781-789.

42. Sui J, Cao W, Halkidis K, et al. Longitudinal assessments of plasma ADAMTS13 biomarkers predict recurrence of immune thrombotic thrombocytopenic purpura. *Blood Adv*. 2019;3(24):4177-4186.

43. Cao W, Krishnaswamy S, Camire RM, Lenting PJ, Zheng XL. Factor VIII accelerates proteolytic cleavage of von Willebrand factor by ADAMTS13. *Proc Natl*

Acad Sci U S A. 2008;105(21):7416-7421.

44. Tarr PI. Shiga toxin-associated hemolytic uremic syndrome and thrombotic thrombocytopenic purpura: distinct mechanisms of pathogenesis. *Kidney Int Suppl*. 2009(112):S29-32.

45. Pickens B, Mao Y, Li D, et al. Platelet-delivered ADAMTS13 inhibits arterial thrombosis and prevents thrombotic thrombocytopenic purpura in murine models. *Blood*. 2015;125(21):3326-3334.

46. Zheng L, Mao Y, Abdelgawwad MS, et al. Therapeutic efficacy of the platelet glycoprotein Ib antagonist anfibatide in murine models of thrombotic thrombocytopenic purpura. *Blood Adv*. 2016;1:75-83.

47. Furlan M, Lammle B. Aetiology and pathogenesis of thrombotic thrombocytopenic purpura and haemolytic uraemic syndrome: the role of von Willebrand factor-cleaving protease. *Best practice & research Clinical haematology*. 2001;14(2):437-454.

48. Ambrose A, Welham RT, Cefalo RC. Thrombotic thrombocytopenic purpura in early pregnancy. *Obstet Gynecol*. 1985;66(2):267-272.

49. Castella M, Pujol M, Julia A, et al. Thrombotic thrombocytopenic purpura and pregnancy: a review of ten cases. *Vox Sang*. 2004;87(4):287-290.

50. Bellart J, Gilabert R, Fontcuberta J, Carreras E, Miralles RM, Cabero L. Coagulation and fibrinolysis parameters in normal pregnancy and in gestational diabetes. *Am J Perinatol*. 1998;15(8):479-486.

51. Clark P, Brennand J, Conkie JA, McCall F, Greer IA, Walker ID. Activated protein C sensitivity, protein C, protein S and coagulation in normal pregnancy. *Thromb Haemost*. 1998;79(6):1166-1170.

52. Zolti M, Ben-Rafael Z, Meirom R, et al. Cytokine involvement in oocytes and early embryos. *Fertil Steril*. 1991;56(2):265-272.

53. Arslan E, Colakoglu M, Celik C, et al. Serum TNF-alpha, IL-6, lupus anticoagulant and anticardiolipin antibody in women with and without a past history of recurrent miscarriage. *Arch Gynecol Obstet*. 2004;270(4):227-229.

54. Lee BE, Jeon YJ, Shin JE, et al. Tumor necrosis factor-alpha gene polymorphisms in Korean patients with recurrent spontaneous abortion. *Reprod Sci*.

2013;20(4):408-413.

55. Brinkmann V, Reichard U, Goosmann C, et al. Neutrophil extracellular traps kill bacteria. *Science*. 2004;303(5663):1532-1535.

56. Engelmann B, Massberg S. Thrombosis as an intravascular effector of innate immunity. *Nat Rev Immunol*. 2013;13(1):34-45.

57. Fuchs TA, Brill A, Duerschmied D, et al. Extracellular DNA traps promote thrombosis. *Proc Natl Acad Sci U S A*. 2010;107(36):15880-15885.

58. Ito T. PAMPs and DAMPs as triggers for DIC. *J Intensive Care*. 2014;2(1):67.

59. Drakeford C, O'Donnell JS. Targeting von Willebrand Factor-Mediated Inflammation. *Arterioscler Thromb Vasc Biol*. 2017;37(9):1590-1591.

60. Rossaint J, Herter JM, Van Aken H, et al. Synchronized integrin engagement and chemokine activation is crucial in neutrophil extracellular trap-mediated sterile inflammation. *Blood*. 2014;123(16):2573-2584.

61. Zirka G, Robert P, Tilburg J, et al. Impaired adhesion of neutrophils expressing Slc44a2/HNA-3b to VWF protects against NETosis under venous shear rates. *Blood*. 2021;137(16):2256-2266.

62. Jimenez-Alcazar M, Napirei M, Panda R, et al. Impaired DNase1-mediated degradation of neutrophil extracellular traps is associated with acute thrombotic microangiopathies. *J Thromb Haemost*. 2015;13(5):732-742.

63. de Buhr N, Parplys AC, Schroeder M, et al. Impaired Degradation of Neutrophil Extracellular Traps: A Possible Severity Factor of Elderly Male COVID-19 Patients. *J Innate Immun*. 2022;14(5):461-476.

64. Lee YY, Park HH, Park W, et al. Long-acting nanoparticulate DNase-1 for effective suppression of SARS-CoV-2-mediated neutrophil activities and cytokine storm. *Biomaterials*. 2021;267:120389.

65. Leffler J, Gullstrand B, Jonsen A, et al. Degradation of neutrophil extracellular traps co-varies with disease activity in patients with systemic lupus erythematosus. *Arthritis Res Ther*. 2013;15(4):R84.

66. Leffler J, Martin M, Gullstrand B, et al. Neutrophil extracellular traps that are not degraded in systemic lupus erythematosus activate complement exacerbating

the disease. *J Immunol*. 2012;188(7):3522-3531.

67. Gollomp K, Sarkar A, Harikumar S, et al. Fc-modified HIT-like monoclonal antibody as a novel treatment for sepsis. *Blood*. 2020;135(10):743-754.

68. Schauer C, Janko C, Munoz LE, et al. Aggregated neutrophil extracellular traps limit inflammation by degrading cytokines and chemokines. *Nat Med*. 2014;20(5):511-517.

69. Leung HHL, Perdomo J, Ahmadi Z, et al. NETosis and thrombosis in vaccine-induced immune thrombotic thrombocytopenia. *Nat Commun*. 2022;13(1):5206.

70. Guimaraes-Costa AB, Nascimento MT, Wardini AB, Pinto-da-Silva LH, Saraiva EM. ETosis: A Microbicidal Mechanism beyond Cell Death. *J Parasitol Res*. 2012;2012:929743.

71. Remijsen Q, Kuijpers TW, Wirawan E, Lippens S, Vandenabeele P, Vanden Berghe T. Dying for a cause: NETosis, mechanisms behind an antimicrobial cell death modality. *Cell Death Differ*. 2011;18(4):581-588.

72. Remijsen Q, Vanden Berghe T, Wirawan E, et al. Neutrophil extracellular trap cell death requires both autophagy and superoxide generation. *Cell Res*. 2011;21(2):290-304.

73. Jarrahi A, Khodadadi H, Moore NS, et al. Recombinant human DNase-I improves acute respiratory distress syndrome via neutrophil extracellular trap degradation. *J Thromb Haemost*. 2023.

74. Ma AC, Kubes P. Platelets, neutrophils, and neutrophil extracellular traps (NETs) in sepsis. *J Thromb Haemost*. 2008;6(3):415-420.

75. Peyvandi F, Scully M, Kremer Hovinga JA, et al. Caplacizumab for Acquired Thrombotic Thrombocytopenic Purpura. *N Engl J Med*. 2016;374(6):511-522.

76. Scully M, Cataland SR, Peyvandi F, et al. Caplacizumab Treatment for Acquired Thrombotic Thrombocytopenic Purpura. *N Engl J Med*. 2019;380(4):335-346.

77. Lei X, Reheman A, Hou Y, et al. Anfibatide, a novel GPIb complex antagonist, inhibits platelet adhesion and thrombus formation in vitro and in vivo in murine models of thrombosis. *Thromb Haemost*. 2014;111(2):279-289.

Figure Legends

Fig. 1. Flow cytometric detection of NETosis in whole blood from patients with iTTP and non-TTP controls. A, **B** and **C**. The gating profiles and the percentage of H3Cit+MPO+ neutrophils (Q2) in unstimulated samples from non-TTP controls, patients with acute iTTP on admission, and those following therapy, respectively. **D**, **E** and **F**. The gating profile and the percentage of H3Cit+MPO+ neutrophils (Q2) in Stx-2-stimulated blood samples from non-TTP controls, iTTP patients on admission, and iTTP patients following therapy, respectively. **G**. Quantitation and statistical analysis of H3Cit+MPO+ neutrophils in unstimulated neutrophil collected from control, iTTP on admission, and iTTP after therapy. **H**. Individual plasma MPO level of patients with acute iTTP and during remission. **I**, **J** and **K** (a paired t-test). The effects of Stx-2 on the percentage of H3Cit+MPO+ neutrophils in non-TTP controls, iTTP patients on admission, and those following therapy, respectively. Kruskal-Willis test was performed in **G** and Mann-Whitney test in **I, J**, and **K**. The data shown are individual values (dots), median (bar), and interquartile range (IQR) (**G, I, J,** and **K**). MPO, myeloperoxidase; Stx-2, Shigatoxin-2; Here, n.s.,*, and ** indicate $p>0.05$, <0.05, and <0.01, respectively.

Fig. 2. Microfluidic assay determines the *ex vivo* thrombus and NETs formation under arterial flow in *vwf*$^{-/-}$ or *Adamts13*$^{-/-}$ mice. A. and **B.** The final mean surface coverage of platelets and leukocytes on a collagen surface and the mean rate of thrombus formation over time, respectively, following a perfusion of a whole blood pre-stimulated with Stx-2 under flow from *vwf*$^{-/-}$ (top) and *WT* (bottom) mice as indicated. **C.** and **D.** The final surface coverage of platelets and leukocytes and the rate of thrombus formation over time, respectively, following a perfusion of a whole

blood pre-stimulated with Stx-2 from *WT* (top) and *Adamts13*$^{-/-}$ (bottom) mice as indicated. **E.** and **F.** Representative confocal microscopic images demonstrate the finally adhered platelets (purple), neutrophils (green), and extracellular DNA strings (elongated green) following a perfusion of whole blood samples from *vwf*$^{-/-}$ vs. *WT*, and WT vs. *Adamts13*$^{-/-}$ mice, respectively. **E'** and **F'** are enlarged (5x) areas from the bottom panels of **E** and **F**, respectively. Here, *WT*, wild type; *a13*$^{-/-}$, *Adamts13*$^{-/-}$; *vwf*$^{-/-}$, vwf null; n, number of mice; N, neutrophil; PLT, platelets. **G**. Quantitation of the number of DNA strings under fluorescent microscope in the blood samples from *vwf*$^{-/-}$, *WT*, and *Adamts13*$^{-/-}$ mice. The data shown in G are individual values (dots), median (bar), and interquartile range (IQR). Kruskal-Wallis test determined the statistical significance among three groups. Here, * indicates $p<0.05$.

Fig. 3. DNase I, recombinant ADAMTS13, and anfibatide inhibit thrombus and prevents NET accumulation under flow in the whole blood of *Adamts13*$^{-/-}$ mice. **A**., **B**., **and C**. The final surface coverage of platelets and leukocytes on a collagen surface following a perfusion of *Adamts13*$^{-/-}$ murine blood samples stimulated with Stx-2 in the presence (top) or absence (bottom) of DNase I (200 IU/mL) or recombinant ADAMTS13 (+rA13) (12 μg/mL), or anfibatide (+ANF) (1.5 μg/mL), respectively, under 100 dyne/cm^2. **D**., **E.,** and **F**. The rate of thrombus formation over time (mean ± SEM) following perfusion of *Adams13*$^{-/-}$ murine blood samples stimulated with Stx-2 in the presence (red) or absence (blue) of DNase I or rA13, or ANF, under flow. **G.**, **H.,** and **I**. Representative confocal microscopic images demonstrate the adhered platelets (purple), neutrophils (green), and extracellular DNA strings (elongated green) at the end of perfusion of whole blood samples from *adamts13*$^{-/-}$ mice, in the presence (top) or absence (bottom) of DNase I, or rA13, or ANF, following fixation and additional staining. **G'., H'.,** and **I'**. Enlarged (5x) areas

from the bottom of panels **G.**, **H.**, and **I.**, respectively, indicate the extracellular DNA strings, platelets, and neutrophils. **J.**, **K.,** and **L**. The number of elongated DNA strings formed at the end of perfusion of blood samples from *Adamts13*$^{-/-}$ mice in the presence or absence of DNase I, rA13, and ANF (n=3), respectively. The data are shown median (bar) and IQR. Mann-Whitney test was used for the differences between the two groups. rA13, recombinant ADAMTS13; ANF, anfibatide; N, neutrophil; PLT, platelet; SEM, standard error of the mean; ** indicates p<0.01.

Fig. 4. Platelets are required for the formation of NETs under flow in whole blood samples of acute iTTP. A. and **B.** Representative images illustrate adhered neutrophils and platelets on a collagen-coated surface following a perfusion of a whole blood sample from iTTP patients on admission and after therapy, respectively, with or without DNase I (200 IU/mL) as indicated. **C.** and **D.** The rate of thrombus formation as a function of time (mean ± SEM, n=6) following a perfusion of iTTP blood samples collected on admission and after therapy, respectively, with or without DNase I (200 IU/mL) as indicated. **E.** and **F**. Final platelets, leukocytes and DNA strings on a collagen surface following a perfusion, fixation, and re-stained with anti-CD41 APC and SytoxGreen with or without DNase I as indicated. **E'. and F'**. Enlarged (5x) areas of the bottom images in **E.** and **F.**, respectively, indicate the extracellular DNA strings, platelets (PLT), and neutrophils (N). **G.** and **H**. The number of DNA strings formed on a collagen surface following perfusion of a blood samples collected from iTTP patients on admission and during remission, respectively, with or without DNase I. The data are shown in median (bar) and IQR. Mann-Whitney test was used to determine the differences. Here, N, neutrophil; PLT, platelet; n.s. and ** indicate p>0.05 and <0.01, respectively.

Fig. 5. Recombinant ADAMTS13 prevents NET formation under flow in iTTP. A. and **B**. Representative images illustrating the final coverage of neutrophils and platelets on a collagen-coated surface following a perfusion of whole blood samples from iTTP on admission and after therapy, respectively, with or without recombinant ADAMTS13 (6 μg/mL) under flow. **C.** and **D**. The rate of thrombus formation (mean ± SEM) as a function of time after a perfusion of whole blood samples of iTTP on admission and following treatment, respectively, with or without rADAMTS13 under flow. **E.** and **F**. Representative confocal fluorescent images show platelets (purple), neutrophils (green), and extracellular DNA strings (elongated green) following a perfusion of whole blood samples from iTTP on admission and following therapy, respectively, with or without rADAMTS13, following fixation and re-staining. **E'.** and **F'**. Enlarged areas (5x) from **E.** and **F.**, respectively, indicate the extracellular DNA strings, platelets, and neutrophils. **G.** and **H**. The number of elongated DNA strings formed at the end of perfusion of whole blood samples from iTTP on admission and following therapy, respectively, with or without rADAMTS13 (n=5). The data shown are median (bar) and IQR. Mann-Whitney test was used for the differences. n.s. and ** indicate $p>0.05$ and <0.01, respectively. Here, rA13, recombinant ADAMTS13; N, neutrophil; PLT, platelet; SEM, standard error of the mean.

Fig. 6. Caplacizumab also prevents the formation of NETs under flow in iTTP. A. and **B**. Representative images illustrating the final coverage of neutrophils and platelets on a collagen-coated surface following a perfusion of whole blood samples from iTTP on admission and after therapy, respectively, with or without caplacizumab (3 μg/mL). **C.** and **D**. The rate of thrombus formation (mean ± SEM) (n=3) as a function of time in the blood samples of iTTP on admission and after treatment, respectively, under flow with or without caplacizumab. **E.** and **F**. Representative

microscopic images show the staining of platelets (purple), neutrophils (green), and extracellular DNA strings (elongated green) following a perfusion of whole blood samples from iTTP on admission and following therapy, respectively, with or without caplacizumab, after fixation and re-staining with anti-CD41 and SytoxGreen. **E'.** and **F'**. Enlarged areas (5x) from the **E.** and **F.**, respectively, indicate the extracellular DNA strings, platelets, and neutrophils. **G.** and **H**. The number of elongated DNA strings (mean ± SEM) (n=3) formed at the end of perfusion of whole blood samples from iTTP patients on admission and after treatment with or without caplacizumab. The data shown are median (bar) and IQR. Mann-Whitney test was used for the differences between two groups. Here, Capla, caplacizumab; N, neutrophil; PLT, platelet; n.s. and ** indicate $p>0.05$ and <0.01, respectively.

Fig. 7. A proposed model of action for DNase I, recombinant ADAMTS13, and caplacizumab to inhibit NET and thrombus formation under flow. **A**. Under flow, VWF is released from endothelial cells (EC) upon stimulation and remains anchored on the endothelial surface, which captures flowing platelets and neutrophils. The neutrophils undergo NETosis and release histone-DNA and histone-MPO complexes (NETs), which bind VWF and activate platelets to enhance thrombus formation. **B**. Whether extracellular DNA strings are degraded by DNase I, VWF strings are removed by rA13, or platelet-VWF interactions are inhibited by Capla or ANF, the result is to destabilize the thrombus structure, dampening inflammation, and thrombosis under flow. N, neutrophil; PLT, platelet; EC, endothelial cell; rA13, recombinant ADAMTS13; Capla, caplacizumab; ANF, anfibatide.

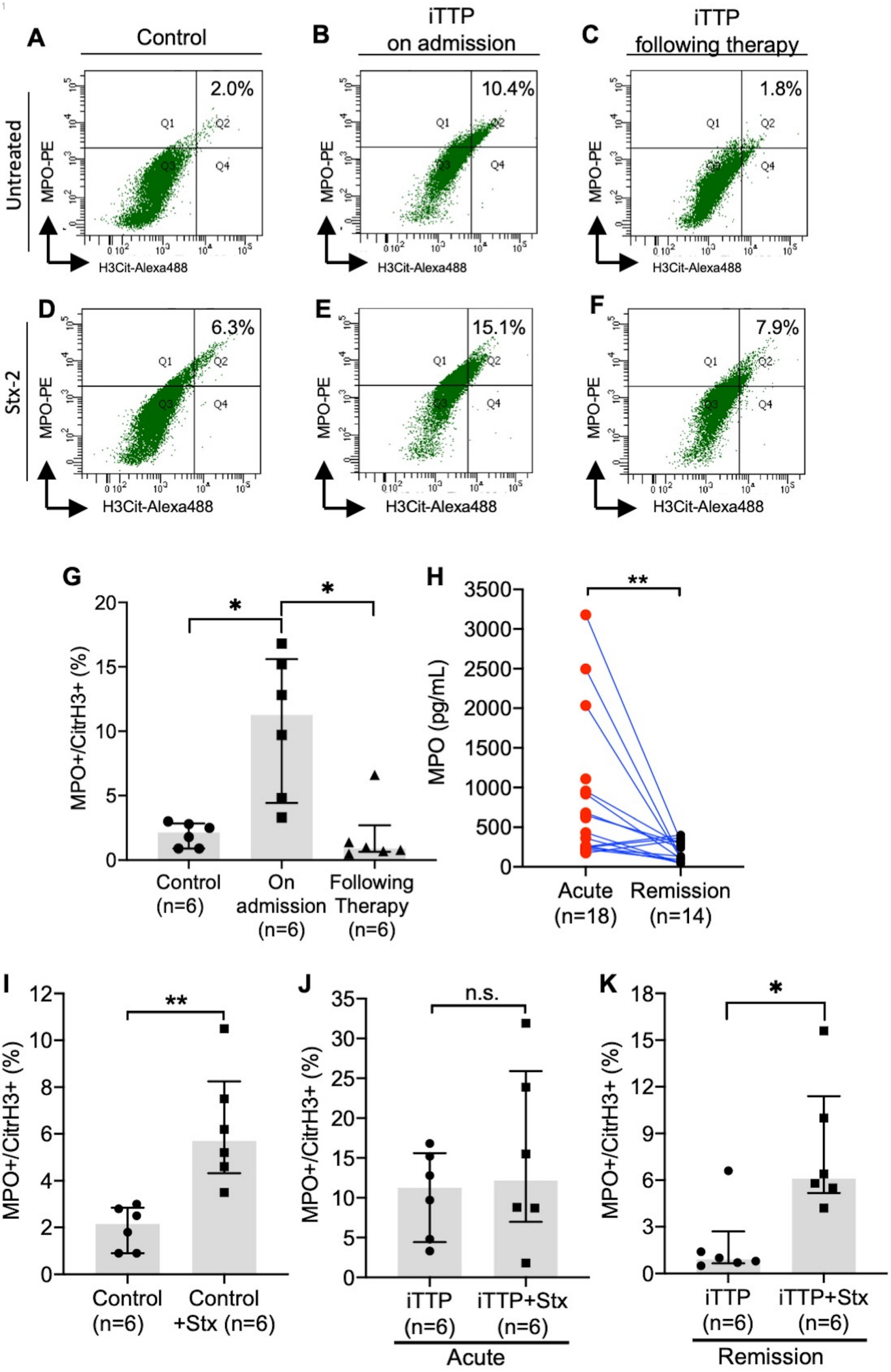

Figure 1

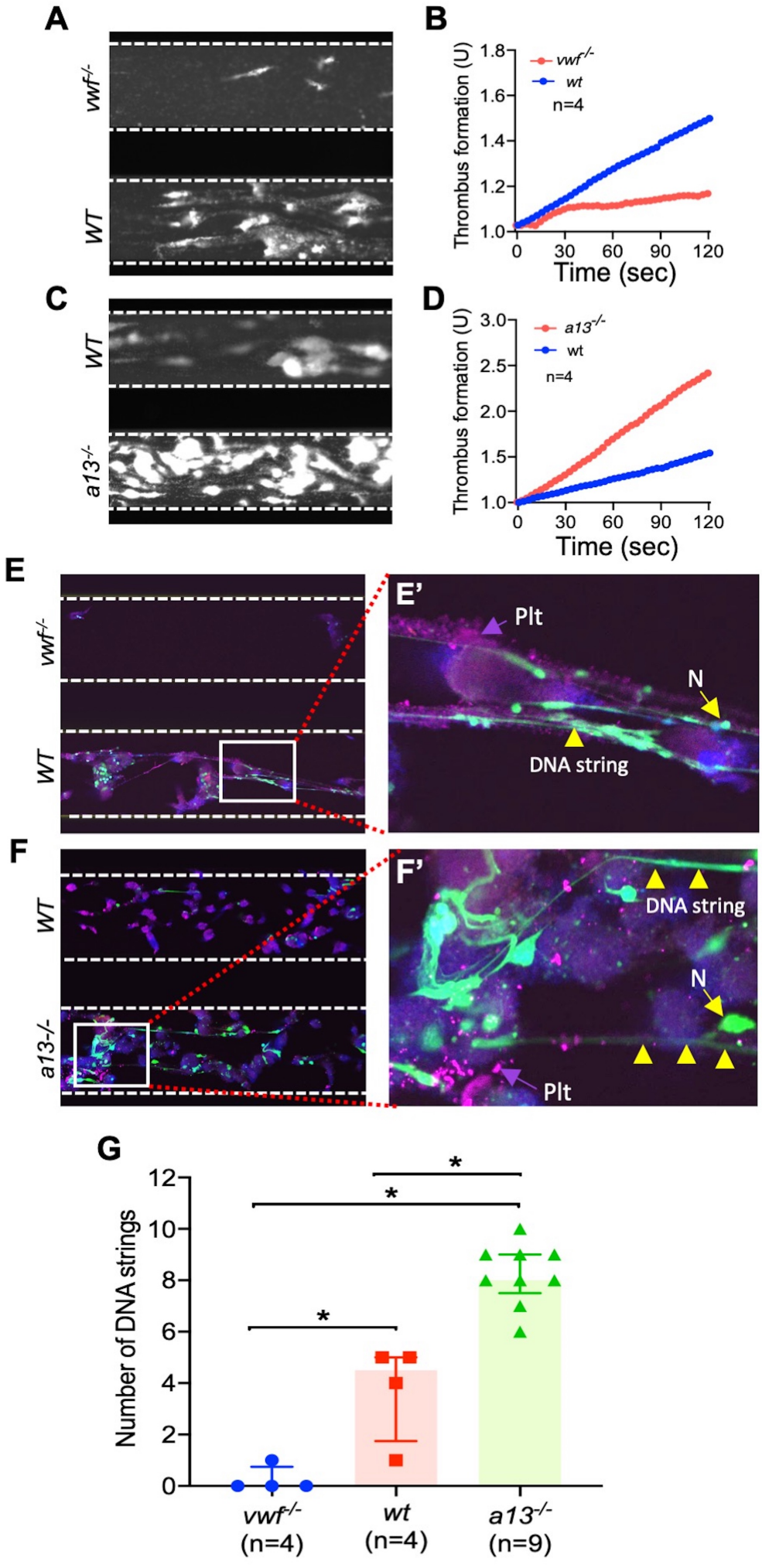

Figure 2

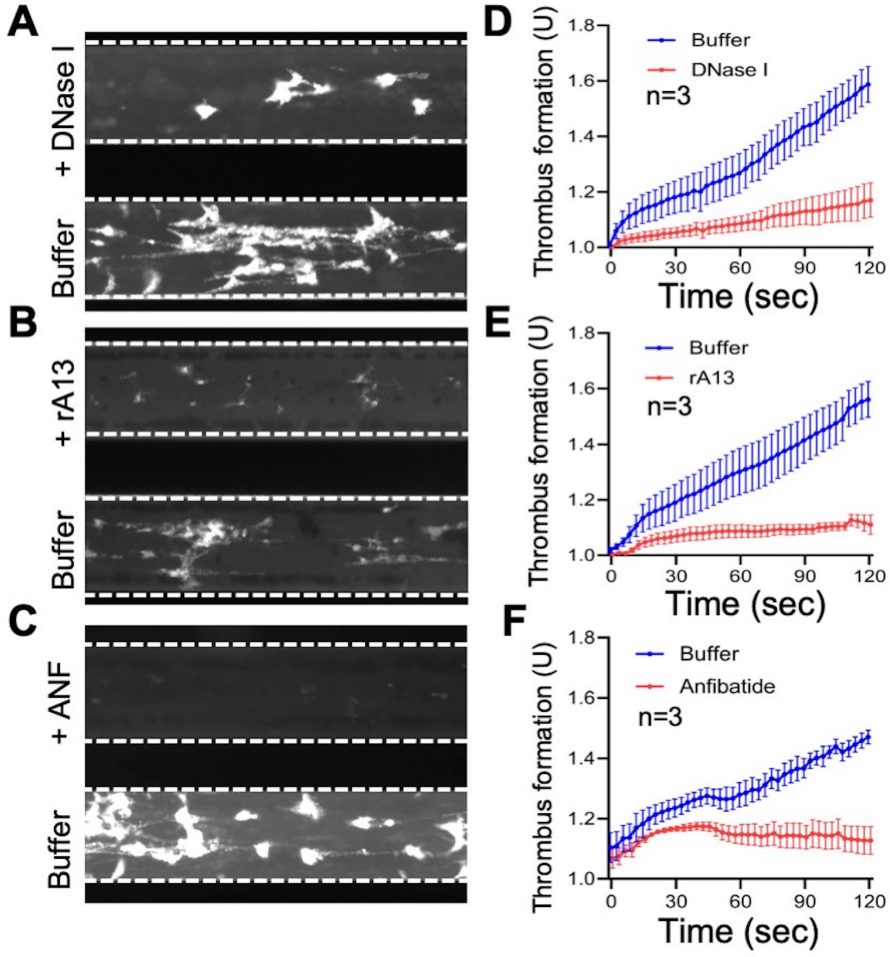

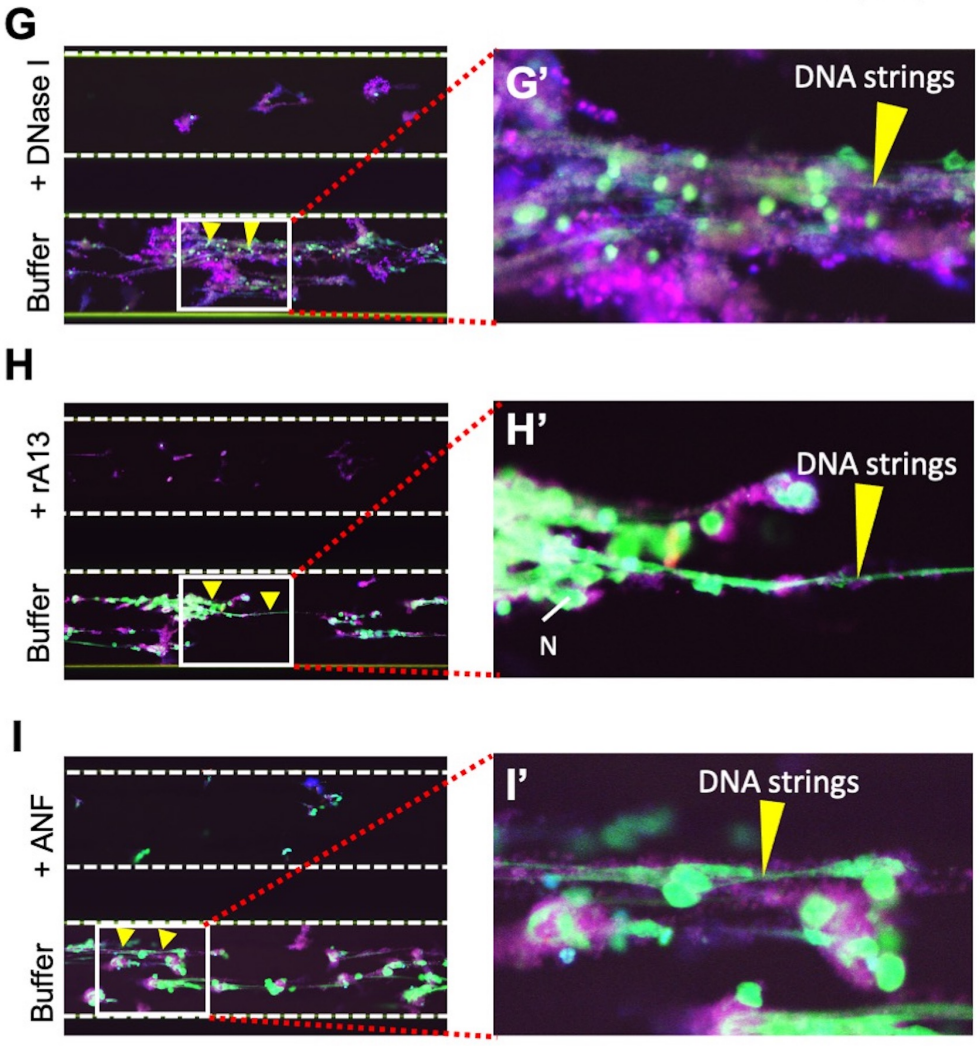

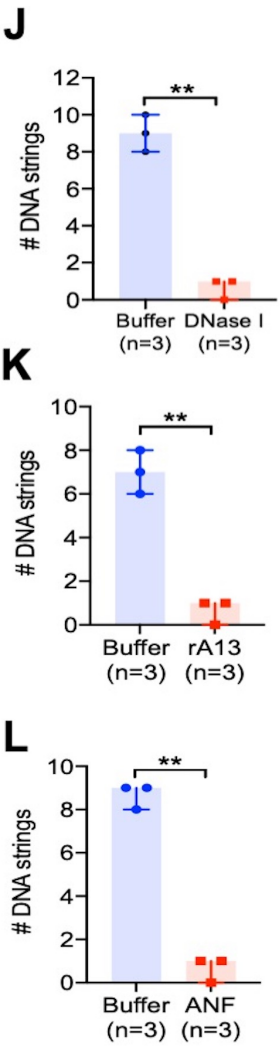

Figure 3

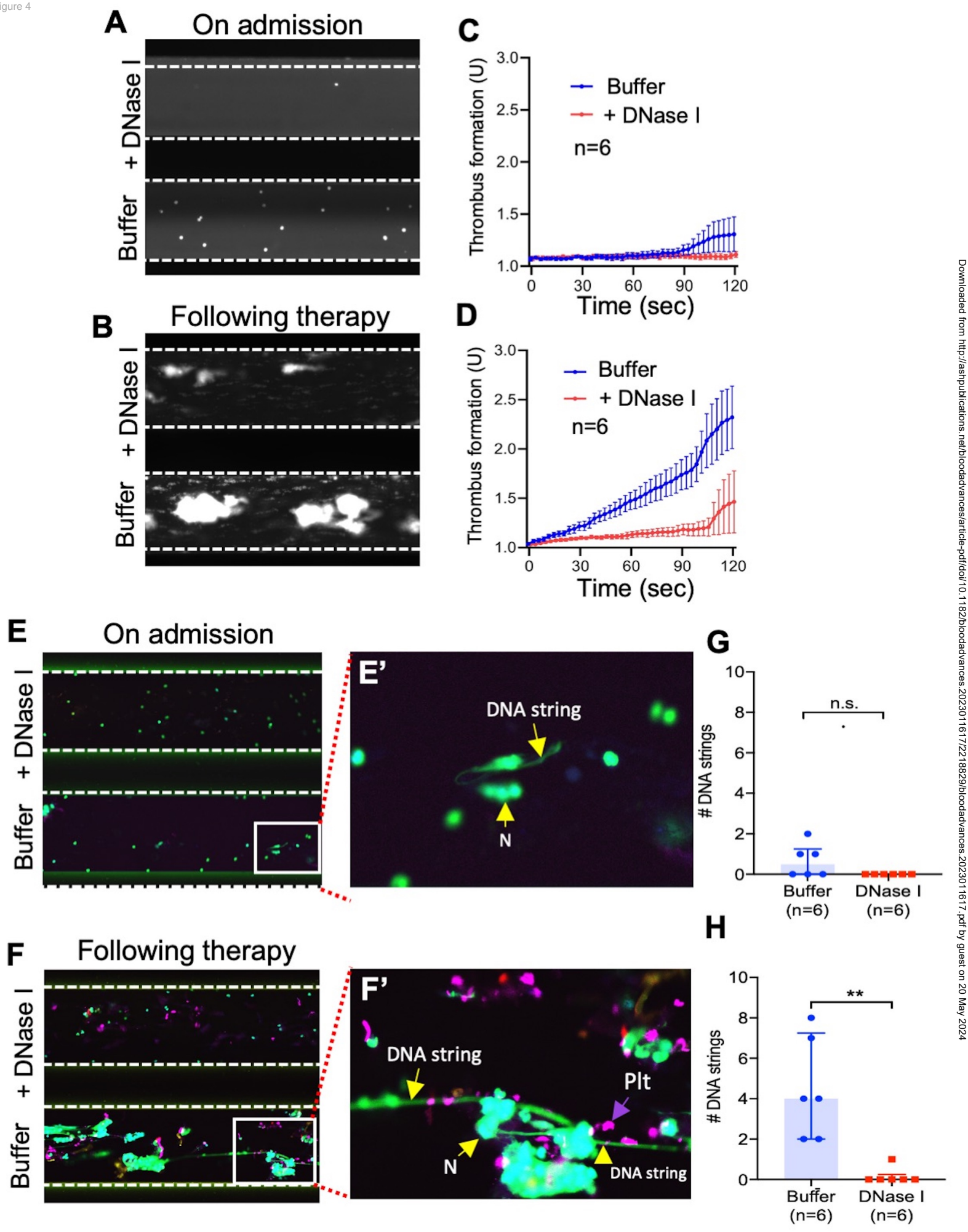

Figure 4

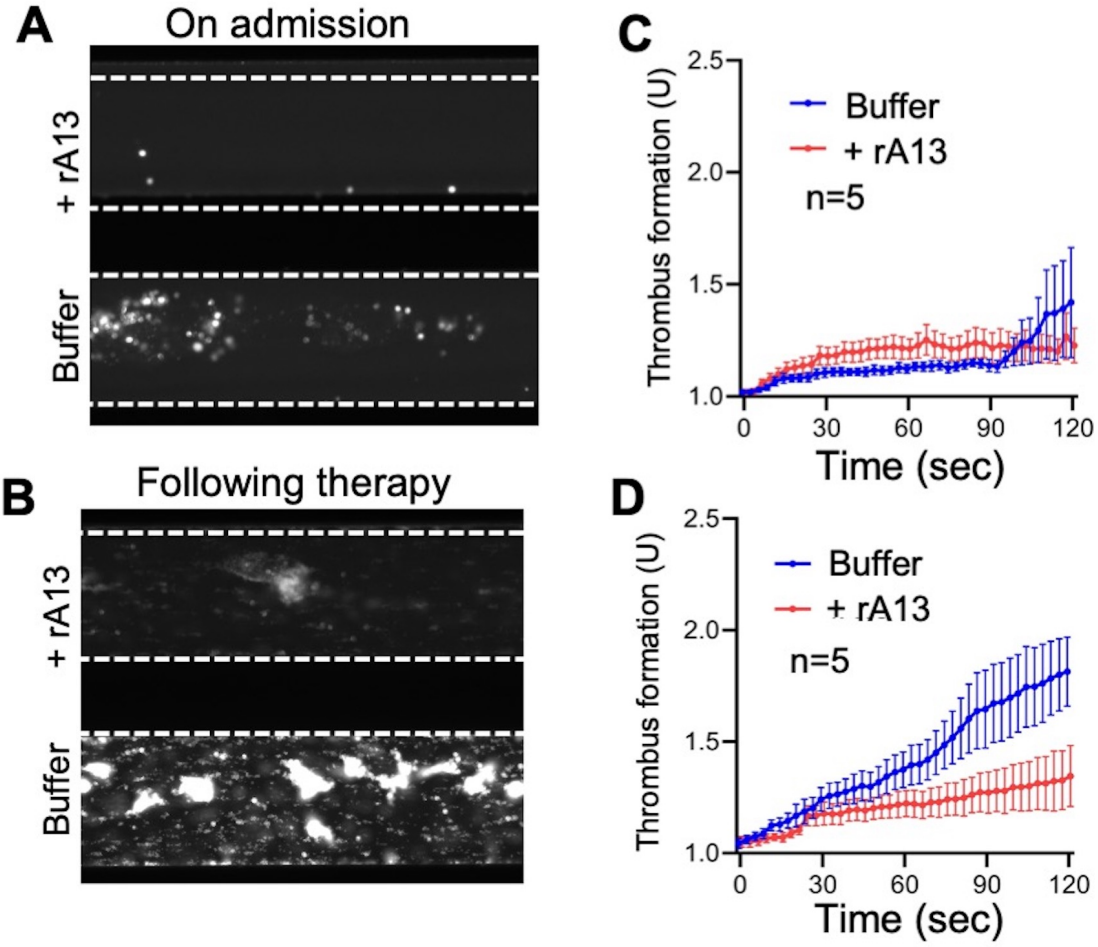

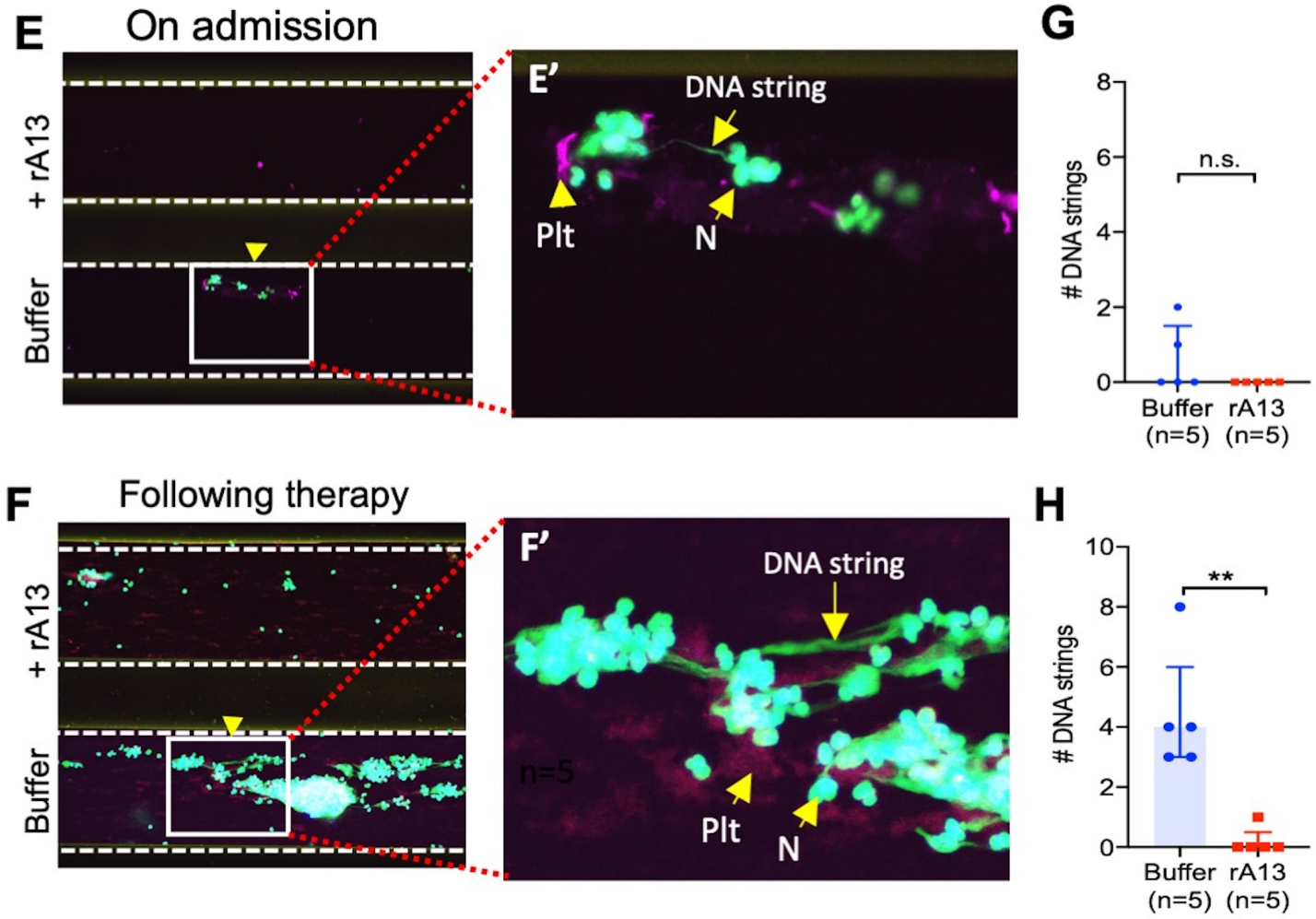

Figure 5

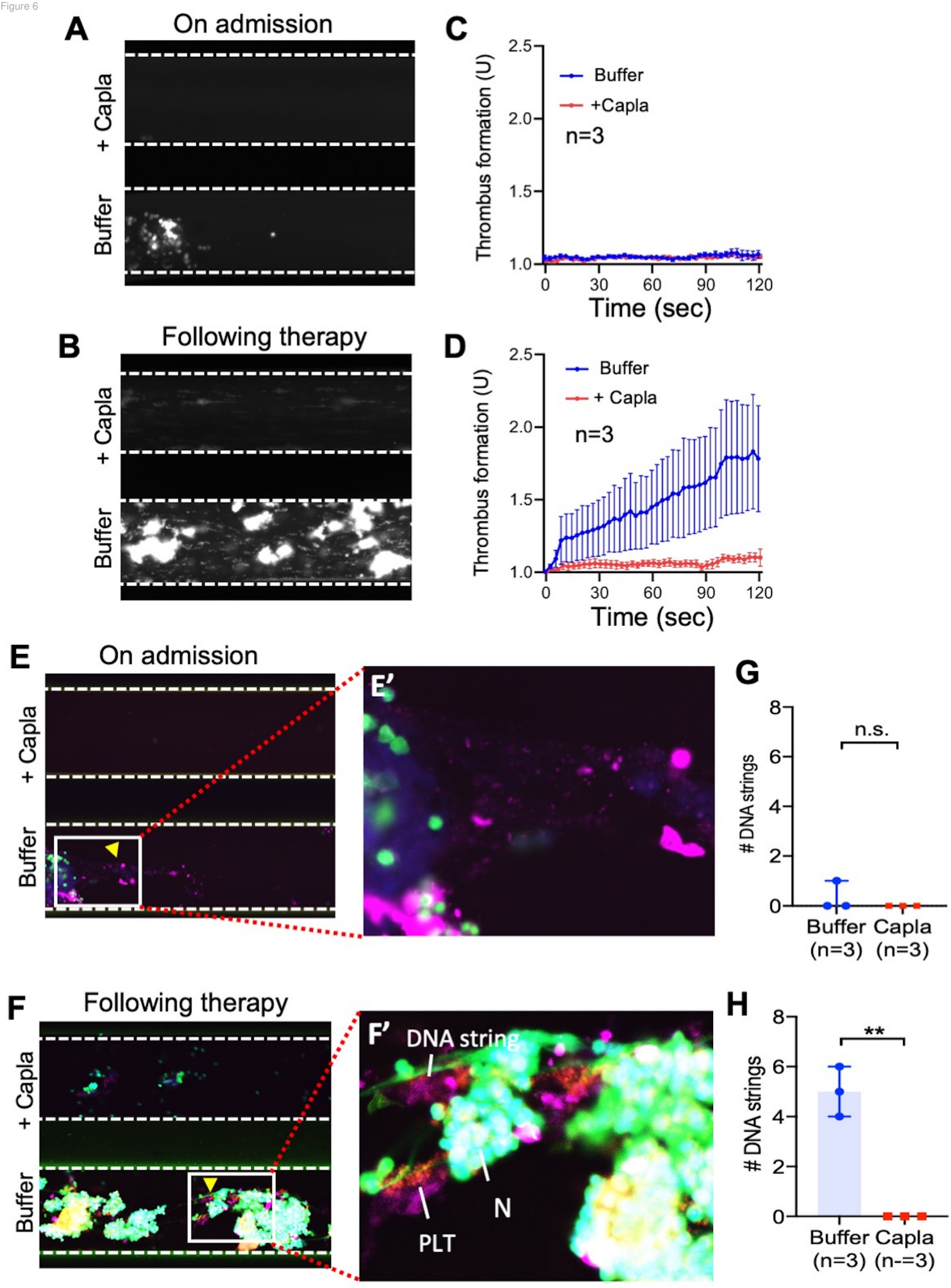

Figure 6

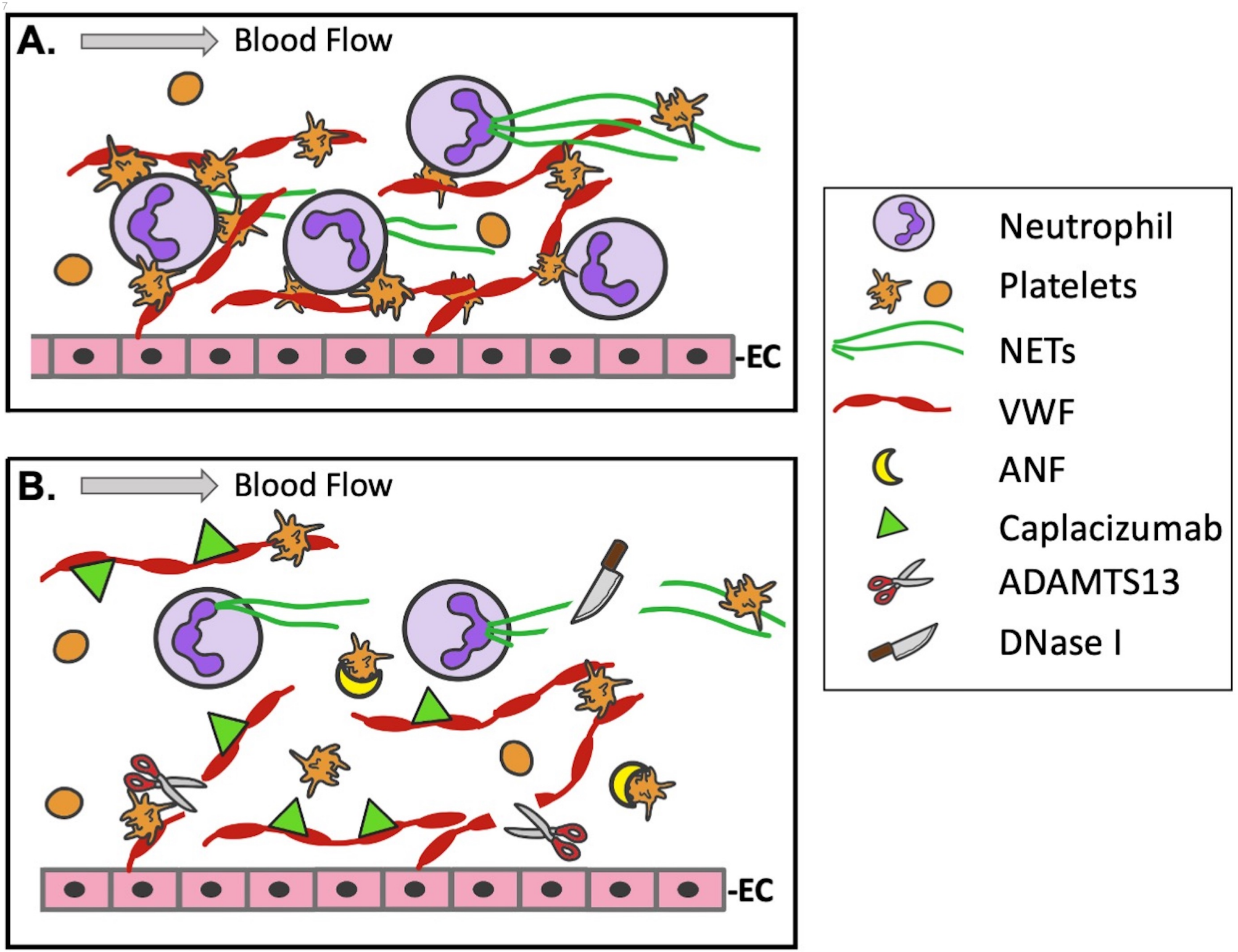

Figure 7